PROCEEDINGS, 47th Workshop on Geothermal Reservoir Engineering
Stanford University, Stanford, California, February 7-9, 2022
SGP-TR-223

Estimating Stress from Fracture Injection Tests: Comparing Pressure Transient Interpretations with In-Situ Strain Measurements

Yves Guglielmi[1], Mark McClure[2], Jeffrey Burghardt[3], Joseph P. Morris[4], Thomas Doe[5], Pengcheng Fu[4], Hunter Knox[3], Vince Vermeul[3], Tim Kneafsey[1], and The EGS Collab Team*

yguglielmi@lbl.gov; mark@resfrac.com

1. Lawrence Berkeley National Laboratory, Berkeley, California, USA
2. ResFrac Corporation, Palo Alto, California, USA
3. Pacific Northwest National Laboratory, Richland, Washington, USA
4. Lawrence Livermore National Laboratory, Livermore, California, USA
5. TDoe Geo, Bellevue, Washington, USA

Keywords: DFIT, minifrac, SIMFIP, Collab

ABSTRACT

The EGS Collab project is a mesoscale project performed at 1.25 and 1.5 km depth at the Sanford Underground Research Facility. A series of fracture injection tests and flow tests have been performed at two different locations within the facility. The tests involved cycles of injection at pressures above the minimum principal stress with fracture opening and propagation, followed by extended shut-in periods. The tests were instrumented with the SIMFIP tool, a double-packer probe with a high-resolution three-dimensional borehole displacement sensor. The tool allows direct observation of strain as the fractures open and close during the tests. These strain measurements can be correlated with pressure measurements to provide high fidelity, direct measurements of fracture closure and reopening, and thus, the minimum principal stress. Typically, in practical applications, only pressure measurements are available from injection/shut-in tests. Different methods to estimate stress from shut-in pressure transients have been proposed in the literature, and sometimes they yield meaningfully different results. Thus, because of the difficulty of validating these different proposed interpretation methods, stress measurement interpretations are sometimes ambiguous and/or debatable. The SIMFIP measurements provide an uncommon opportunity to test these proposed pressure transient methods against direct physical measurements. In this study, we compare the SIMFIP measurements against four extended shut-in pressure transients from the EGS Collab project. The shut-in transients were analyzed with two different techniques – the 'tangent' method and the 'compliance' method. In three of the four tests, the tangent method significantly underestimated the minimum principal stress. The compliance method was reasonably accurate in all four tests.

1. INTRODUCTION

1.1 Background

Accurate measurement of stress in the subsurface is foundational to the field of geomechanics. Fracture injection testing is the most widely-used approach for estimating the magnitude of the minimum principal stress (Hubbert and Willis, 1957; Godbey and Hodges, 1958; Kehle, 1964; Haimson and Fairhurst, 1967; Hickman and Zoback, 1983; Zoback, 2007; Schmitt and Haimson, 2017). Fluid is injected at a rate that is high compared with the rock's capacity to accommodate flow. This results in a high pressure that typically creates

* J. Ajo-Franklin, T. Baumgartner, K. Beckers, D. Blankenship, A. Bonneville, L. Boyd, S. Brown, J.A. Burghardt, C. Chai, A. Chakravarty, T. Chen, Y. Chen, B. Chi, K. Condon, P.J. Cook, D. Crandall, P.F. Dobson, T. Doe, C.A. Doughty, D. Elsworth, J. Feldman, Z. Feng, A. Foris, L.P. Frash, Z. Frone, P. Fu, K. Gao, A. Ghassemi, Y. Guglielmi, B. Haimson, A. Hawkins, J. Heise, C. Hopp, M. Hom, R.N. Horne, J. Horner, M. Hu, H. Huang, L. Huang, K.J. Im, M. Ingraham, F. Jafarov, R.S. Jayne, T.C. Johnson, S.E. Johnson, B. Johnston, S. Karra, K. Kim, D.K. King, T. Kneafsey, H. Knox, J. Knox, D. Kumar, K. Kutun, M. Lee, D. Li, J. Li, K. Li, Z. Li, M. Maceira, P. Mackey, N. Makedonska, C.J. Marone, E. Mattson, M.W. McClure, J. McLennan, T. McLing, C. Medler, R.J. Mellors, E. Metcalfe, J. Miskimins, J. Moore, C.E. Morency, J.P. Morris, T. Myers, S. Nakagawa, G. Neupane, G. Newman, A. Nieto, T. Paronish, R. Pawar, P. Petrov, B. Pietzyk, R. Podgorney, Y. Polsky, J. Pope, S. Porse, J.C. Primo, T. Pyatina, C. Reimers, B.Q. Roberts, M. Robertson, V. Rodríguez-Tribaldos, W. Roggenthen, J. Rutqvist, D. Rynders, M. Schoenball, P. Schwering, V. Sesetty, C.S. Sherman, A. Singh, M.M. Smith, H. Sone, E.L. Sonnenthal, F.A. Soom, D.P. Sprinkle, S. Sprinkle, C.E. Strickland, J. Su, D. Templeton, J.N. Thomle, C. Ulrich, N. Uzunlar, A. Vachaparampil, C.A. Valladao, W. Vandermeer, G. Vandine, D. Vardiman, V.R. Vermeul, J.L. Wagoner, H.F. Wang, J. Weers, N. Welch, J. White, M.D. White, P. Winterfeld, T. Wood, S. Workman, H. Wu, Y.S. Wu, E.C. Yildirim, Y. Zhang, Y.Q. Zhang, Q. Zhou, M.D. Zoback

an opening mode crack that propagates into the formation. For the crack to open against the Earth's stress, the fluid pressure must exceed the minimum principal stress.

In order for a crack to propagate, the fluid pressure must be sufficiently high to drive the crack though the rock. The 'net pressure' is the difference between the crack's internal pressure during propagation and the minimum principal stress. Linear elastic fracture mechanics predicts that net pressure should be small (100 psi or less) for a crack larger than a few meters. However, empirical data suggests that net pressure is often on the order of hundreds of psi (Shylapobersky, 1985; Section 6-7.2 from Mack and Warpinski, 2000). This could occur if scale-dependent processes cause in-situ, effective fracture toughness to be higher than measured in the laboratory (Delaney et al., 1986; Scholz, 2010). The fracture toughness is related to the energy (or equivalently, stress intensity factor) required to propagate the crack through the rock. Processes such as inelastic deformation ahead of the crack tip could elevate this energy consumption compared to purely elastic-brittle deformation.

To account for the possibility of nonnegligible net pressure, the 'closure pressure' can be estimated from a fracture injection test. The idea is to analyze the pressure transient after shut-in to identify when the fracture walls touch. This is taken as an estimate for the minimum principal stress.

1.2 Estimating stress from shut-in pressure transients

Schmitt and Haimson (2017) describe various methods for estimating stress from shut-in data after a fracture injection test. A common technique is to plot pressure versus the square root of time, and then pick closure (and the stress estimate) at the point of deviation from a straight line (Zoback, 2007). If the fracture is assumed to be created instantaneously, the leakoff rate from the fracture is expected to scale approximately with the inverse of the square root of time, and so if the fracture stiffness is constant prior to closure, a plot of pressure versus square root of time should generate a straight line.

To account for non-instantaneous crack propagation during injection, Nolte (1979) developed the 'G-function.' The G-function is a function of time, somewhat analogous to the square root of time, defined such that the cumulative volume of fluid leaked off after shut-in is proportional to the G-function. It is expected that prior to closure, a plot of pressure versus G-time should make a straight line (Castillo, 1987). The theoretical basis for these approaches is described in Section 2.1.

Barree et al. (2009) introduced a substantially different set of recommendations, which became widely adopted in the petroleum industry and will be named here as the "tangent method." In the petroleum industry, fracture injection tests are often called 'diagnostic fracture injection tests' (DFIT). Barree et al. (2009) recommend making a plot of G*dP/dG and drawing a straight line from the origin to the tangent to the curve. The pressure at this point in time is used as an estimate for the minimum principal stress.

McClure et al. (2016; 2019) used numerical modeling and analytical derivations to argue that the tangent method systematically underestimates the magnitude of the minimum principal stress and consequently overestimates the net pressure. They introduced a step-by-step interpretation procedure called the 'fracture compliance method.' With some minor differences, the procedure is fairly analogous to the classical 'deviation from linearity' method. McClure et al. (2016; 2019) explained why shut-in transients are qualitatively different in high and low permeability formations and designed a recommended interpretation procedure specifically for low permeability formations (ie, lower than 10-20 microdarcy). The tangent method and compliance method are described in Section 2.1.

McClure et al. (2022) statistically compared 'tangent method' and 'compliance method' stress estimates from 51 fracture injection tests performed in shale plays across North and South America. The estimates varied by 100-1250 psi, with an average difference of 444 psi. Both methods suggested that net pressure can be on the order of hundreds of psi, supporting the theory that toughness is elevated at field scale. However, the tangent method net pressure estimates were on average 2.5 times higher, implying much shorter, wider fractures with much greater effective toughness.

Because of these discrepancies, there is a need for experiments in which the pressure transient interpretations are compared against independent measurements.

1.3 Other examples in the literature

Dutler et al. (2020) compared G-function interpretations from the Grimsel project to in-situ strain measurements and found that the tangent method consistently underestimated the closure stress, and that compliance-based interpretations were accurate. These tests mostly exhibited a monotonic dP/dG response, a special case for the compliance method that is discussed in Section 2.1 below.

McClure et al. (2016) compared strain measurements from the DOE M-Site project to G-function interpretations. They found that the compliance method yielded an accurate stress measurement, and that the tangent method underestimated the closure response.

In contrast, Craig et al. (2017) compared strain measurements from the DOE M-Site project and from laboratory experiments and concluded that the results supported the use of the tangent method interpretations. McClure (2019) critically analyzed their interpretations and concluded that their study had technical and methodological flaws. For example, Craig et al. (2017) did not use the 'x-intercept' approach explained in Section 2.1 (figure 9A-4 from Gulrajani et al., 2001), but instead tried to identify reopening near the first perceptible deflection from zero.

Malik et al. (2014) analyzed microfrac tests performed from vertical wells in shale. They did not use downhole strain measurements, but because the well is vertical (so that there is no expectation of near-wellbore tortuosity), the reopening pressures from the injections can

be compared with the closure estimates and assessed for consistency. The dP/dG plots were monotonically decreasing, suggesting either an ambiguous or 'rapid closure' compliance method interpretation. Because there is no expectation of near-wellbore tortuosity, the 'rapid closure' interpretation would be the best compliance method interpretation (discussed in Section 2.1 below). The reopening pressures suggest that the 'rapid closure' interpretation is most accurate, and that the tangent method consistently underestimates the stress.

Bröker and Ma (2022) compared five different stress estimation methods from a series of minifrac injections. They found that the tangent method yielded results systematically much lower than the other four techniques and that the results were in some cases so low that they exceeded the frictional limit of the rock mass. The compliance method results were the second lowest, but much more similar to the other techniques than the tangent method, and did not violate frictional equilibrium.

1.4 Approach used in this study

In this study, we compare the 'tangent' and 'compliance' method closure interpretations against direct, in-situ strain measurements.

The SIMFIP tool (Step-Rate Injection Method for Fracture In-Situ Properties) is based on a double packer hydrofracturing probe customized with a 6-component displacement sensor that is integrated in the injection interval sealed between the two packers (Figure 1; Guglielmi et al., 2013). The injection interval is 2.41 m long (Figure 1). The displacement sensor is set in the center of the interval. It is a 0.24 m long and 0.1 m diameter pre-calibrated aluminum cage that is connected to two 0.58 m long elements that allow clamping both ends of the cage on the borehole wall (clamps correspond to points A and B in Figure 1). When it is clamped, the cage is disconnected from the straddle packer system. Thus, during an injection test, it captures the relative borehole wall displacement between the upper and the lower anchor which are 1.4 m away. Note that the distance between the two anchors is shorter than the injection interval length. When a fracture is activated, the SIMFIP sensor captures the three-dimensional displacement without any influence from the packer system. The packers are used to seal the test interval. The resolution of the SIMFIP measurement is estimated around the micrometer level. The range of the measurements is a few millimeters. During a SIMFIP test, there is a continuous and synchronous measurement of oriented three-dimensional borehole wall displacements, injection pressure, and flowrate.

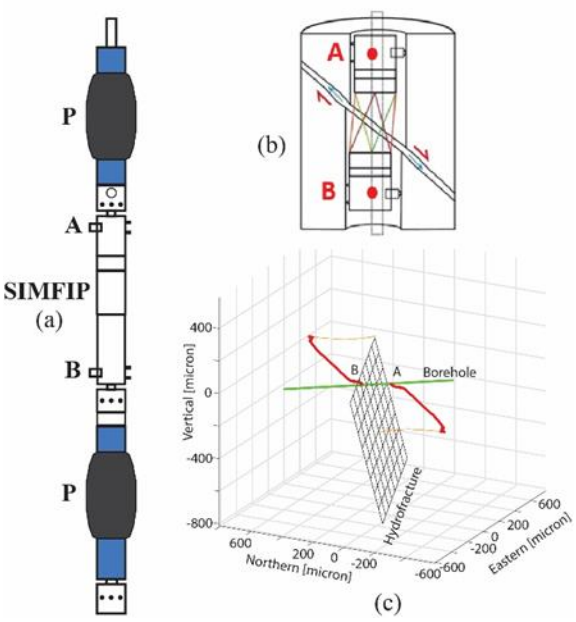

Figure 1: SIMFIP probe. (a) Design of the probe; (b) Schematic concept of the borehole three-dimensional relative displacement between anchors A and B ; (c) Example of a SIMFIP displacement signal captured across the activated hydrofracture during E1-I 164 Test 2. Red segment is the displacement during injection and growth of the fracture. Orange segment is the displacement during shut-in.

To be included in this study, shut-in tests had to meet the following criteria: (a) a shut-in period of at least a few hours, (b) SIMFIP measurements taken during the injection and shut-in cycle, and (c) the injection did not cause a fracture that intersected and drained into a neighboring borehole. We analyze the only four injection sequences from the Collab project that met these requirements. One possible exception: the E1-I 164 Test 2 was included even though the fracture probably had a slight leakage into a grouted, neighboring observation well, as discussed below.

The measurements were taken in 2018 and 2019 during hydrofracturing experiments that took place in boreholes that were drilled from drifts at the 4850' and 4100' levels of the mine, which are approximately 1,490.5 m and 1250 m below ground surface (BGS), respectively. The borehole on the 4850 level, E1-I, was 69 m long and slightly dipping from horizontal while the 4100 borehole, TV 4100, was approximately 50 m long and vertical. Both boreholes were drilled in fractured metamorphic rocks of the Sanford Underground Research Facility (SURF) in South Dakota, USA (Kneafsey et al., 2019, 2020; Guglielmi et al., 2021). The E1-I test used here was the second

stimulation of a zone at a measured depth of feet 50 m (or E1-I 164 ft) which, and we refer to as the E1-I 164 Tests. The TV 4100 tests were performed at measured depths between 10 and 45 meter measured depth and these are referred to by test number, TV 4100 Test 4, and TV 4100 Test 7.

In the E1-I 164 tests (~1490.5 m BGS), the vertical stress magnitude is estimated to be ~41.8 MPa based on the density of overlying rocks. The subhorizontal intermediate and minimum principal stresses SHmax and Shmin have previously been estimated to be 34.0 and ~21.7 MPa (Kneafsey, 2020; Kneafsey et al., 2020; Singh et al., 2019; Wang et al., 2017). The pore pressure and magnitude of Shmin may have significant spatial variability because of differential drainage of fluid over time into the neighboring mineshaft. The borehole is drilled subparallel to the estimated Shmin. The injection zone's geology is intact foliated metamorphic rock (Poorman Formation).

The E1-I 164 Tests consisted of three propagation and shut-in steps, each step extending the fracture further into the rock until it intersected a borehole located 10 m away from the injection well. Each step, named 1, 2, and 3 in this paper, provided fracture opening and shut-in records. Using the continuous borehole displacements monitored with the SIMFIP probe, it appeared that micro-shearing of the borehole initiated on a foliation plane until injection pressure increased to 112% of the estimated Shmin, triggering the opening and sliding of a new hydrofracture. SIMFIP displacements allowed defining a hydrofracture average orientation consistent with induced seismic events alignment and with the intersection location in the monitoring borehole (Figure 1). Using simple modeling, a mixed mode of fracture growth best matched the measurements, in accordance with the ambient normal stress regime (Guglielmi et al., 2021; Schoenball et al., 2020; Fu et al., 2021).

In the TV 4100 tests, the same SIMFIP probe was used. Eight SIMFIP tests were conducted to monitor fracture displacement response at different depths along the 50 m deep borehole to build a stress profile and to characterize the stress variability along this profile. In addition, other stress measurement techniques such as conventional hydraulic testing (leakoff tests) and new thermal fracturing techniques were tested in the same borehole with some test intervals overlapping between the techniques. The tests intervals selected in this study are set in foliated ambhibolite affected by cemented natural fractures. Indeed, one objective of the SIMFIP tests was to probe whether these fractures would activate under pressure or if new hydrofractures would be generated.

The 4100 Test 4 interval contained five natural fractures, apparently all cemented. The 4100 Test 7 interval contained about ten fractures, all apparently cemented. Some contained a several centimeter thick in-filling cement and a centimeter thick damage zone. Comparisons between acoustic logs before and after both tests did not show new fractures. Stronger acoustic contrasts were observed along some segments of preexisting fractures suggesting that these fractures had been reactivated. These observations combined with the measured orientation of the SIMFIP displacements enabled identification of the best candidates for fracture reactivation, as well as the mode of reactivation.

2. METHODS

2.1 Interpretation of shut-in transients

To illustrate the two tangent and compliance interpretation methods, we first show an example from a prior study.

Figure 2 and Figure 3 show an example of a DFIT pressure transient from a horizontal well drilled in the Utica/Point Pleasant shale (figures reproduced from McClure et al., 2019). The blue curve shows pressure, and the red curves show either the magnitude of dP/dG or G*dP/dG.

Very early in the shut-in, pressure drops very rapidly, by over 3000 psi. This part of the transient is ignored because it is caused by dissipation of near-wellbore tortuosity related to the initiation of a transverse hydraulic fracture from a horizontal well. The straight section of the pressure versus G-time plot can be extrapolated back to the y-intercept to estimate the pressure in the far-field fracture at shut-in (the so-called effective initial shut-in pressure). In Figure 2, the effective ISIP is 8330 psi. After the initial period, the pressure curve settles into an approximately straight line.

The straight line ends at a G-time of approximately 17 (at around 8100 psi), as the pressure curve begins to drop more rapidly (i.e., the magnitude of dP/dG increases). The ‘compliance method’ of estimating stress identifies the contact pressure at the point where the derivative has increased from the minimum and subtracts 75 psi to account for stress shadow from residual aperture (McClure et al., 2019). This yields a ‘compliance method’ stress estimate of 8025 psi. The 75 psi adjustment is based on numerical simulation matches to field DFITs (McClure et al., 2019). Nevertheless, it is somewhat arbitrary, and this reflects the uncertainty that is inherent to stress measurements.

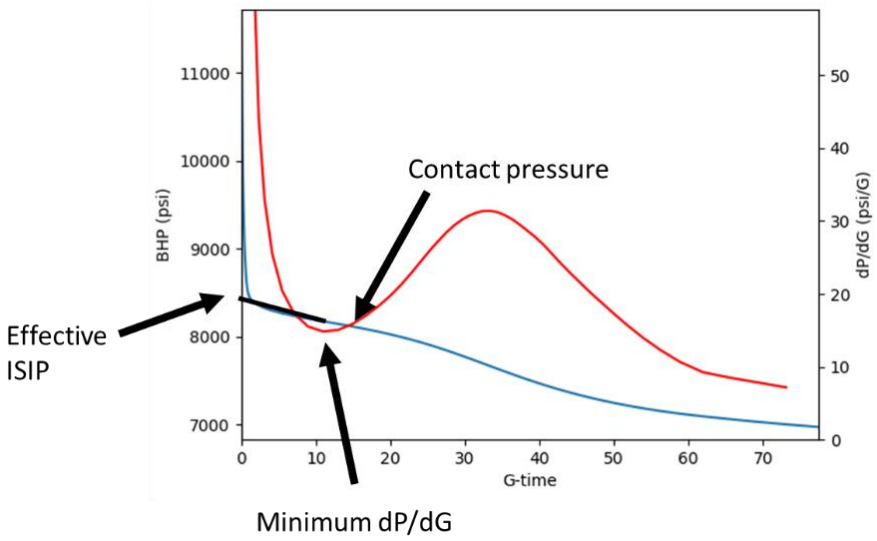

Figure 2: Example of a compliance method stress estimate. The blue curve shows pressure, and the red curve shows dP/dG. Data taken from a fracture injection test in the Utica/Point Pleasant Shale.

The tangent method for estimating stress is taken from a plot of G*dP/dG. A straight line is drawn from the origin to the tangent to the curve. The pressure at this point in time is taken as the tangent method stress estimate. In Figure 3, the tangent method stress estimate is 7630 psi, 395 psi lower than the compliance method estimate. The net pressure (the effective ISIP minus the stress estimate) is 700 psi with the tangent method and 305 psi with the compliance method. The tangent method was developed to match numerical simulations by Barree and Mukherjee (1996) and Barree et al. (2009).

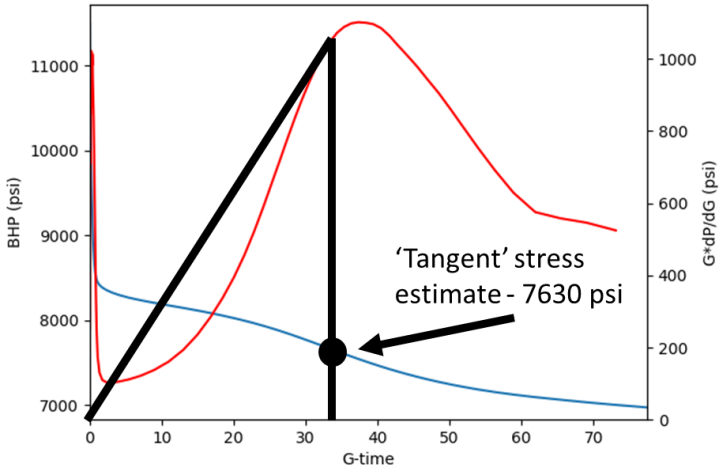

Figure 3: Example of a tangent method stress estimate. The blue curve shows pressure, and the red curve shows G*dP/dG. Data taken from a fracture injection test in the Utica/Point Pleasant Shale.

The compliance method for estimating stress was developed from mathematical solutions of the fracture closure process (McClure et al., 2016). When fracture walls contact during closure, this impacts fracture stiffness and fracture conductivity. If the permeability is sufficiently low (as in shale), the fracture remains effectively infinite in conductivity by comparison, even after closure, and the fracture can be approximated as having a uniform internal pressure. Under these conditions, it is possible to derive (McClure et al., 2016; 2019):

$$\frac{dP}{dG} = \frac{1}{C_t}\frac{dV}{dG}, \tag{1}$$

where P is pressure, G is G-time, C_t is the storage coefficient of the wellbore/fracture system, and V is the volume of fluid in the wellbore/fracture system. The storage coefficient is defined as the volume of fluid released from the system per increment of pressure decrease. It combines the effect of both changing fluid density and changing system volume as a function of pressure.

Prior to closure, the system storage coefficient is approximately constant (Sneddon, 1946; Equation 9-21 from Gulrajani and Nolte, 2001; Section 8.13 from Jaeger et al., 2007). Furthermore, from the derivation of the G-function (Nolte, 1979), until the pressure in the fracture has dropped substantially, dV/dG is approximately constant. Therefore, at early time (after the near-wellbore tortuosity period), pressure versus G-time forms an approximately straight line. When the fracture walls contact, the stiffness increases, and the storage coefficient drops. This causes dP/dG to increase when the fracture walls contact.

McClure et al. (2016, 2019) note that because of the roughness of the fracture walls, the fluid pressure may be slightly higher than the minimum principal stress when the walls contact. Based on numerical simulations designed to closely match field data, they recommend estimating stress as 75 psi lower than the contact pressure. The contact pressure is estimated by plotting the magnitude of dP/dG and identifying the point where this derivative reaches a minimum and begins to increase. This is the so-called 'compliance' method stress estimate. With some nuanced differences, the 'compliance method' is close to the classical method of picking closure at the deviation from linearity.

An upward deflection in dP/dG is not always seen in the shut-in transients. Sometimes, dP/dG decreases continuously during shut-in. McClure et al. (2019) discussed possible causes of the lack of an upward deflection. One possibility is excessive near-wellbore tortuosity. If the fluid pathway pinches off during shut-in and isolates the wellbore from the far-field fracture, it may not be possible to interpret the data. A second possibility is that the fracture closes almost immediately after shut-in.

In either case, monotonically decreasing dP/dG arises from processes that create a time-dependent spatial pressure gradient between the well and the fracture. Equation 1 relies on the assumption of an infinitely conductive fracture system with spatially uniform pressure. If pressure is not uniform, and transient effects occur within the system, the behavior predicted by Equation 1 need not occur.

More speculatively, monotonic dP/dG might arise from continued crack growth after shut-in. However, for such growth to occur for longer than a few minutes, processes such as subcritical crack growth would need to be invoked.

In vertical wells, when near-wellbore tortuosity is usually minimal (because the crack is more prone to initiate from the wellbore at its far-field orientation), McClure et al. (2019) recommends interpreting tests with monotonic dP/dG as indicating 'rapid closure,' and so the stress estimate should be within several hundred psi of the ISIP. However, in tests where near-wellbore tortuosity is possible, McClure et al. (2019; 2022) recommends declining to provide a stress estimate and labeling the stress uninterpretable. Ambiguity between the effect of near-wellbore tortuosity and rapid closure makes confident interpretation impossible in this case.

In a review of 62 field DFITs performed in shale formations (10-100 barrels of injection), McClure et al. (2021) found that 59% showed a clear upward deflection; 25% showed an adequate upward deflection; and 16% showed no indication of an upward deflection (i.e., a monotonic dP/dG).

Literature review suggests that monotonic dP/dG are more common in tests with lower volume, a few barrels or less (Malik et al., 2014; Dutler et al., 2020; Broker and Ma, 2022). Possibly, this is because small cracks are very stiff and have low aperture, which means that crack roughness may be of similar order of magnitude as the aperture.

McClure et al. (2019) recommend supplementing dP/dG plots with plots of 'relative stiffness' versus pressure. The relative stiffness is an unnormalized value calculated to be proportional to the system stiffness. The relative stiffness plot is useful because the value of dV/dG in Equation 1 will only be constant if leakoff scales with the square root of time. This property no longer holds true once the pressure in the fracture has decreased significantly (more than a few hundred psi) after shut-in. A relative fracture stiffness plot performs a time-convolution of the pressure history in the fracture and calculates a value proportional to the system stiffness, accounting for changes in pressure over time. In cases where dP/dG appears to increase at a significantly lower pressure than the effective ISIP, it can be useful to confirm the apparent change in stiffness from an effective stiffness plot.

For example, Figure 4 shows the relative stiffness versus pressure plot for the same test shown in Figure 2 and Figure 3. There is an upward deflection at 8100 psi, corresponding to the upward increase in dP/dG seen in Figure 2. If 'rapid closure' occurs, then the relative stiffness plot cannot be used to pick closure. This manifests as a non-ideal shape on the relative stiffness plot.

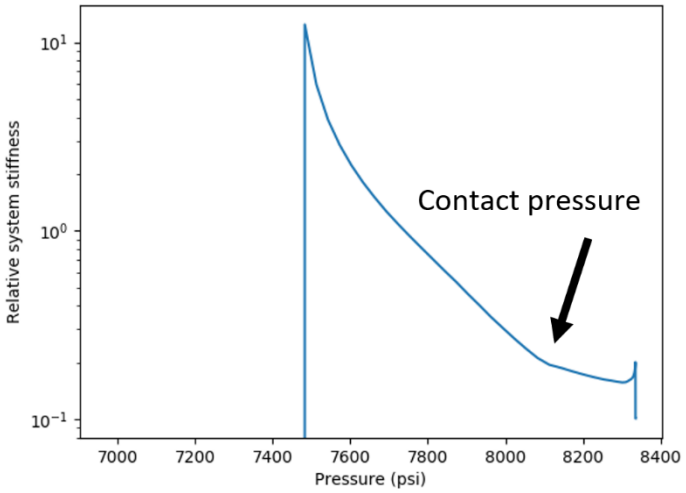

Figure 4: Example of a relative stiffness versus pressure plot. Data taken from the same Utica/Point Pleasant Shale fracture injection test that is shown in the previous figures.

2.2 SIMFIP

A typical SIMFIP test contains several injection cycles. During the first cycle, pressure is increased step by step up to a maximum value that is considered well below the fracturing pressure. Then pressure is stepped down to initial. This cycle is used to characterize the hydromechanical response of the injection chamber that integrates the rock formation mechanical response, the effect of the mechanical coupling of both SIMFIP clamps and packers and the probe's stiffness. Usually, there is a clear and sometimes complex correlation between the borehole displacements and the pressure, and displacements are totally reversible when pressure is stepped back to initial. Then, one or more injection cycles are conducted in order to fracture from the chamber and to grow the fracture away from the borehole. These tests are classical constant flowrate or pressure step rate tests but with borehole displacements measured in addition to pressure and injection flowrate. At the fracturing pressure, the SIMFIP displacements lose the initial correlation to injection pressure, and they start relating to the orientation and activation mode of the created or reactivated fracture. Several stimulation cycles may be necessary to get a clear displacement orientation if there are local borehole tortuosity effects. For example, during the SURF E1-I 164 Test 1 stimulation at 1490.5 m BGS, the nucleation of the fracture initiated by shearing a foliation plane at the borehole wall, and this orientation strongly influenced the displacement measurement at early stages (Guglielmi et al., 2021). Then, with injection time, a sufficiently large macroscopic fracture grew away from the borehole and reoriented perpendicular to the minimum principal stress. The SIMFIP displacement thus starts showing a consistent displacement orientation at the end of the E1-I 164 Test 1 and during E1-I 164 Test 2 which followed, corresponding to a reopening of the initiated hydrofracture.

There are different ways to estimate the stress, depending on the observed SIMFIP displacements and pressure. The best-case scenario is when the SIMFIP displacement vector orientation associated with the activation of an interval fracture can be compared to the activated fracture geometry obtained by comparing the borehole wall acoustic logs before and after the test.

For example, in E1-I 164 Tests 1 and 2, the hydrofracture geometry could be deduced from the alignment of seismic events and from distributed fiber optic temperature and strain data that localized the fracture intersection with adjacent monitoring boreholes.

However, the activated fracture identification is less clear in TV 4100 Tests 4 and 7 where it appears that natural fractures have been reactivated. In such cases, the orientation of the SIMFIP displacement indicates if the activated fracture is between the anchors or outside. Then, it is compared to the mapped natural fractures on the acoustic log for example. In this case, there may be multiple potentially activated natural fractures (Kakurina et al., 2020). The SIMFIP three-dimensional displacement is then converted into a component tangential and normal to the activated fracture. The normal component manifests when the fracture is opening. It can be directly related to the pressure at which this occurs. The shear component can eventually be used to complement the stress tensor estimation, for example by applying a more advanced Coulomb stress inversion (Guglielmi et al., 2020).

Section 9A from Gulrajani and Nolte (2001) explains how to estimate the magnitude of the minimum principal stress from deformation measurements, either during shut-in or reopening. As shown in Figure 5, the rock displacement should be plotted versus pressure.

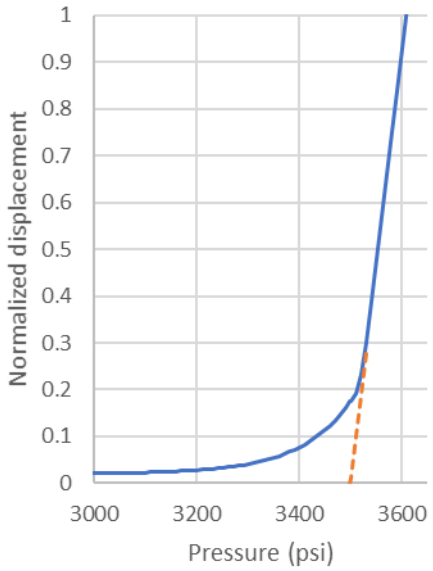

Figure 5: Schematic of hydraulic fracture reopening/closure. Based on Figure 9A-4 from Gulrajani and Nolte (2001). The orange dashed line shows the extrapolation of the 'open fracture' curve back to the minimum principal stress, as per Equation 2.

For a crack perpendicular to the minimum principal stress, when the crack is mechanically open and not propagating, there is an approximately linear relationship between deformation and pressure, as given by the equation (Sneddon, 1946; Equation 9-21 from Gulrajani and Nolte, 2001; Section 8.13 from Jaeger et al., 2007):

$$\overline{W} = \frac{P - Shmin}{S_f} = (P - Shmin)C_f, \quad (2)$$

where $\overline{W}$ is the average fracture width (defined as the crack volume divided by area), S_f is the fracture stiffness, C_f is the fracture compliance (equal to the reciprocal of fracture stiffness), and Shmin is the minimum principal stress.

If reopening a preexisting fracture that is not perpendicular to Shmin, the normal stress on the crack will be higher than Shmin, and the fracture may experience some irreversible shear as the crack opens for the first time. The fracture walls contain asperities that contact during closure, creating a backstress that nonlinearly increases stiffness (Barton et al., 1985). The asperities contact at a width $\overline{W_c}$ that is some fraction of the maximum width reached during injection. If the crack was perfectly smooth, then $\overline{W_c}$ would be equal to zero, and the straight line would extend all the way to zero on the x-axis of Figure 5. With nonzero $\overline{W_c}$, the curve deviates from the straight line and curves to asymptotically approach zero (or possibly, a small residual width) as pressure decreases below Shmin. Equation 2 shows that the x-intercept of the straight line in Figure 5 is equal to Shmin. Thus, as shown by Figure 9A-4 from Gulrajani and Nolte (2001), the x-intercept of the straight line is equal to Shmin. It might be tempting to identify 'closure/reopening' as the point where the displacement visually deviates from zero. However, the progressive, asymptotic reduction in aperture that occurs with pressure falloff continues even as pressure goes well-below Shmin.

Other complex hydromechanical mechanisms influence the SIMFIP displacements. The most common observed ones are:

- During the start of the first injection cycle into an interval, the fracture has not yet formed, and so the deformation versus pressure response cannot be interpreted for stress.
- The fracture activation mode is not pure tensile, and thus some of the opening is related to irreversible shear induced dilation.

3. RESULTS AND DISCUSSION

3.1 E1-I 164 Interval

In E1-I 164 Test 1, injection was performed for 10 minutes at a constant 0.2 l/min flowrate, followed by a 2 hour shut-in. During shut-in, pressure dropped to 22.2 MPa (3220 psi) before a power outage ended the SIMFIP recording (Figure 6). Pressure measurements continued after the SIMFIP measurements ended, reaching a minimum of 20.0 MPa (2900 psi).

In E1-I 164 Test 2, the zone pressure was first held constant at 13.8 MPa for about 5 minutes and then increased to 20.7 MPa for about 1 minute. The protocol was then switched from pressure-controlled to flowrate-controlled. The flow rate was increased in successive steps to a maximum of 0.4 l/min for 57 minutes (Guglielmi et al., 2021). The pressure increased to 26.8 MPa and then decreased to a relatively constant value of 26.7 MPa just before the pump was stopped, and the zone was left shut in for 15 hours (Figure 7).

In E1-I 164 Test 3, injection was performed at 3 l/min until the fracture broke through to an offset production well, as confirmed by visual measurements with a downhole camera in the offset well.

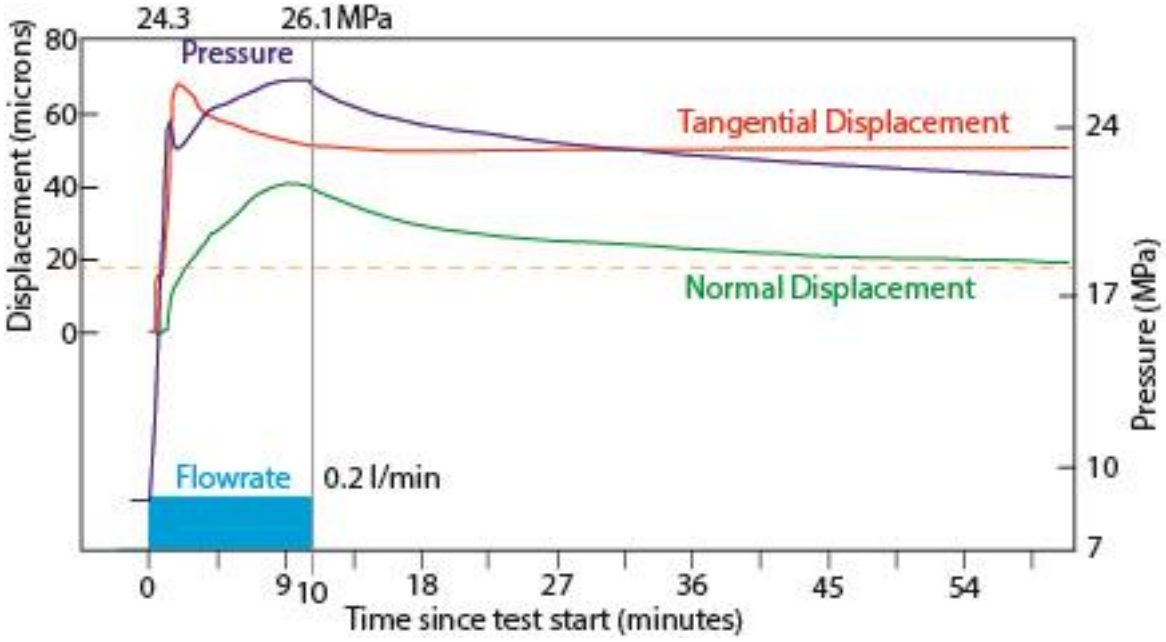

Figure 6: SIMFIP displacement normal and tangential to the activated fracture during E1-I 164 Test 1. Displacements are plotted with injection chamber pressure and injection flowrate (note that only a part of the shut-in is plotted on this graph).

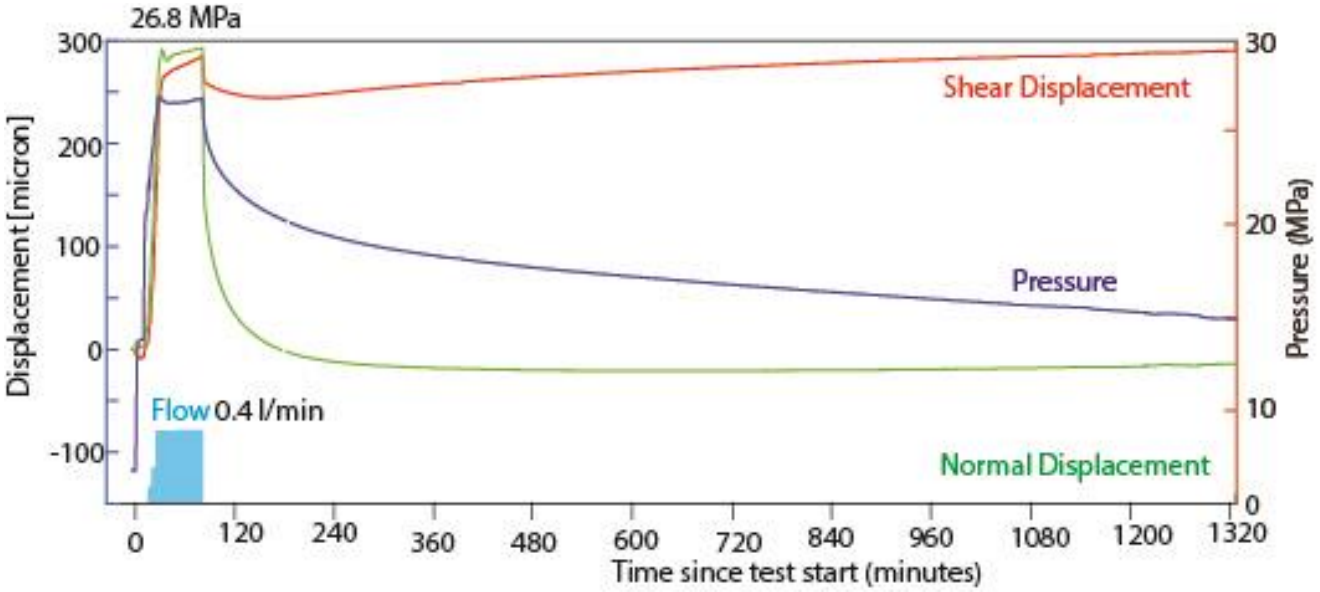

Figure 7: SIMFIP displacement normal and tangential to the activated fracture during E1-I 164 Test 2. Displacements are plotted with injection chamber pressure and injection flowrate.

The SIMFIP measurements from the Test 1 shut-in cannot be used to estimate stress because of the early loss of recording – the measurements did not reach an asymptotic minimum. In Tests 2 and 3, the measured reopening and shut-in displacements lie on top of

each other; each has an x-intercept stress estimate around 21.4 MPa (3100 psi). The deformation continues to asymptotically approach its limiting value as pressure drops further below 3100 psi, indicating the gradual closure of the fracture after the walls have contacted.

As seen in Test 3, the final asymptote of the displacement need not occur exactly at zero. Irreversible shear displacement of the rock during the injection can cause an apparent offset from zero, as measured from the beginning of injection. Thus, the displacement data from the Test 1 shut-in cannot be interpreted to estimate stress using the technique shown in Figure 5, because we do not know the location of the final asymptote in displacement. The bending of the curve suggests that it may have occurred at a y-axis value around 30 microns, implying an 'x-intercept' at around 21 MPa, similar to Tests 2 and 3. However, without the measurements, this is not known with certainty.

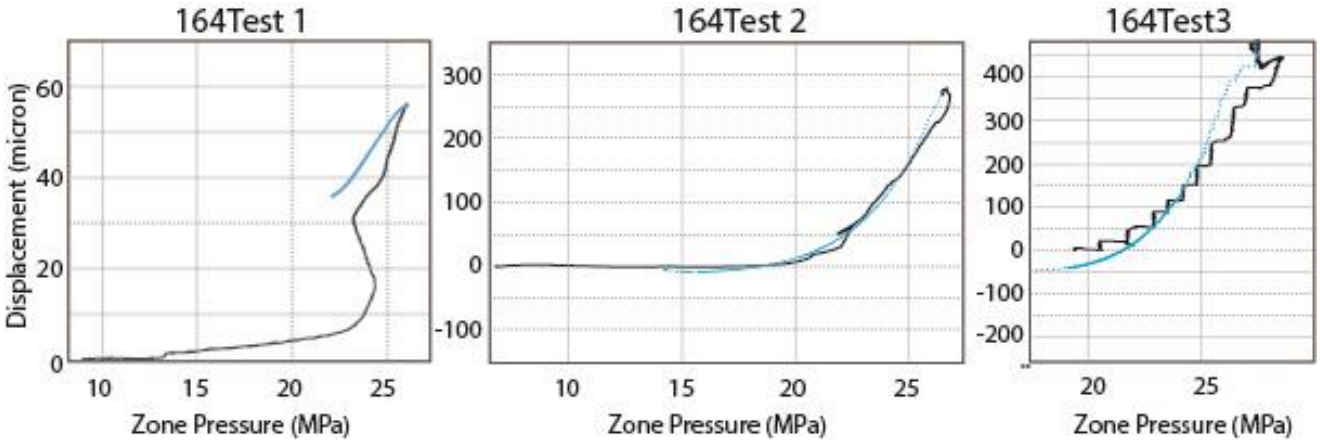

Figure 8: SIMFIP displacement normal to the activated fracture versus zone pressure for the E1-I 164 tests (Black is the injection period, blue is the shut-in period).

Figure 9 shows dP/dG, G*dP/dG, and relative stiffness plots from the first injection cycle in the E1-I 164 interval. The dP/dG plot rises up from a minimum, implying a contact pressure of 3175 psi and a stress estimate of 3100 psi. Correspondingly, the relative stiffness plot shows an upward inflection at 3200 psi. On the other hand, the tangent method interpretation is that the fracture did not close by the end of the transient, reaching 2900 psi.

The compliance stress estimate of 3100 psi is close to the x-intercept stress estimates from the SIMFIP measurements. The tangent method is at least 200 psi lower, and it may have been much lower if the transient had continued longer.

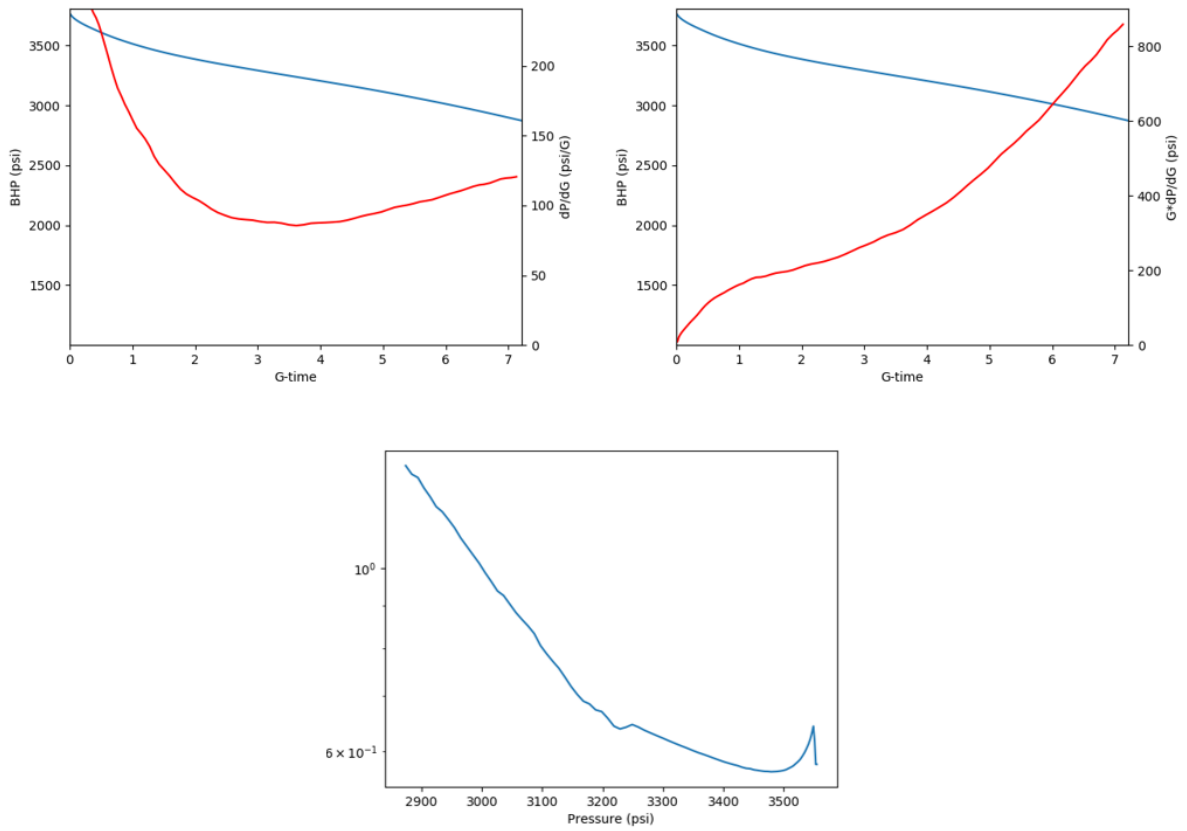

Figure 9: dP/dG, G*dP/dG, and relative stiffness plots for E1-I 164 Test 1.

In the second injection cycle, the dP/dG curve is monotonically decreasing (Figure 10). There is little indication of near-wellbore tortuosity, and so the McClure et al. (2019) 'compliance' interpretation is that the fracture closed relatively quickly. The relative stiffness plot has a non-ideal shape, consistent with the interpretation that the fracture closed relatively quickly, and so the closure process cannot be described by Equation 1. The 'rapid closure' interpretation from McClure et al. (2019) implies a significant error bound on the stress estimate - anywhere from 3000-3500 psi.

The G*dP/dG curve continues increasing and does not reach a tangent by the end of the test, reaching a minimum pressure of 2200 psi. Therefore, the tangent method interpretation is that the fracture never closed and that the stress is lower than 2200 psi.

The SIMFIP estimate of 3100 psi is within the vicinity of the (fairly wide and uncertain) range of stress estimates from the 'rapid closure' interpretation. The tangent interpretation is far too low, and it would have been even lower if the shut-in had continued for longer.

During E1-I 164 Test 2 shut-in, a small DTS response was observed in a neighboring observation well. This is interpreted as indicating that the observation well was hit by one of the fractures. The observation well was grouted, but it is nevertheless possible that some fluid from the fracture leaked into the well. This may have impacted the transient by accelerating leakoff.

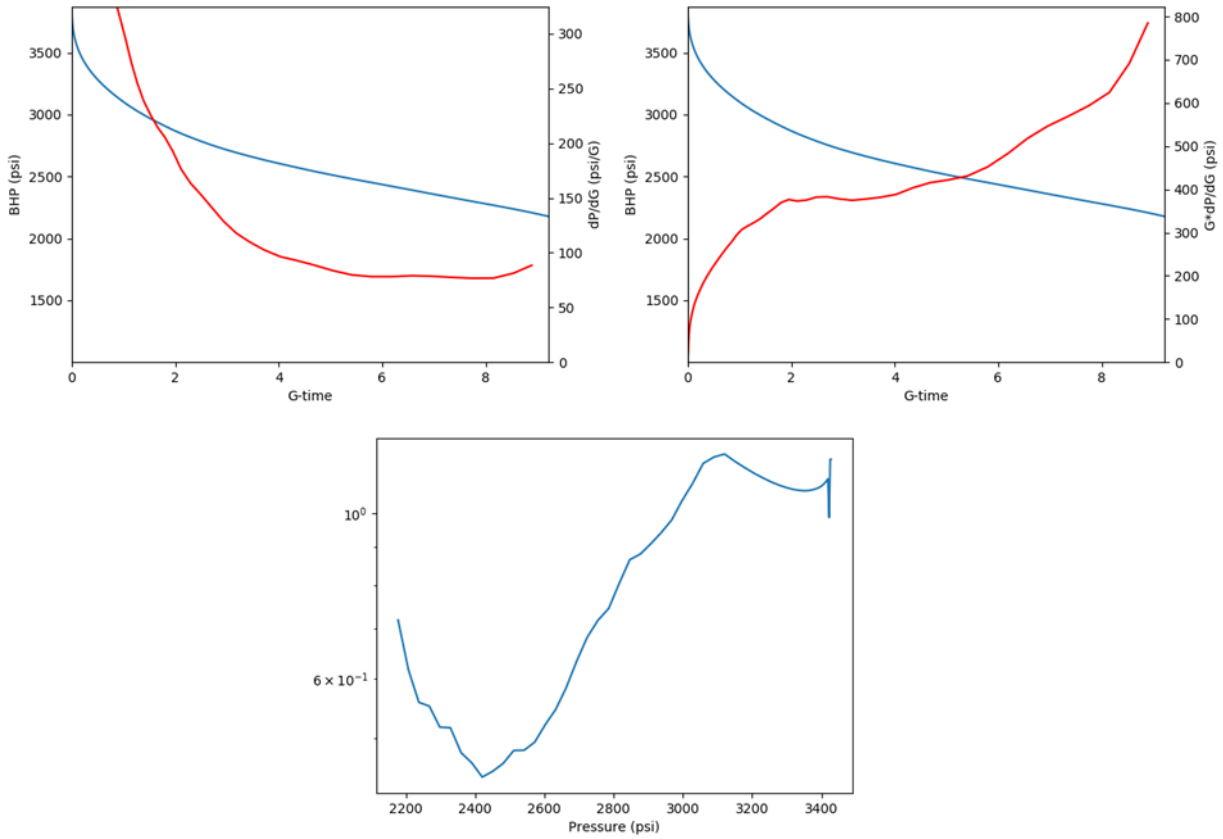

Figure 10: dP/dG, G*dP/dG, and relative stiffness plots for E1-I 164 Test 2.

3.2 TV 4100 Interval

In the two tests in the TV 4100 interval, injection reactivated natural fractures at the wellbore, rather than directly propagating a hydraulic fracture. This causes the SIMFIP measurements to be more complex than in the E1-I 164 tests.

In TV 4100 Test 4, a constant 1.2 l/min flowrate injection was conducted for 10:29 minutes before a 7-hours long shut-in (Figure 11). The SIMFIP measurements indicate reactivation of a cemented natural fracture set between the two SIMFIP anchors with approximate orientation of 236°/54° dip direction/dip angle. At the fracturing pressure during injection, a complex displacement response is observed, characterized by displacement tangential to the fracture associated with closing. Then, at 2:21 minutes after injection, the fracture starts opening with a limited normal displacement of about 5 microns. At shut-in there is a strong instantaneous tangential displacement and a smooth normal closure.

The SIMFIP estimates of closure in Cycle 1 and reopening in Cycle 2 are affected by nonmonotonic behavior evidently caused by complex hydromechanical effects associated with leakage into the formation. During the Cycle 1 shut-in, the normal displacement drops to near zero at 19 MPa (2785 psi), and then goes back up. Estimates of stress from the x-intercept are challenging because the data does not yield a smooth, ideal straight-line, as in the E1-I 164 tests. In Cycle 2, the best estimate for reopening pressure is 18.7 MPa (2712 psi).

The TV 4100 interval Test 4 transient reaches a minimum dP/dG and rises back up, yielding a contact pressure of 2550 psi and a stress estimate of 2475 psi. Correspondingly, the relative stiffness plot shows an upward deflection at approximately 2500 psi The G*dP/dG curve is still bending upwards at the end of the transient, and so the tangent method interpretation is that the fracture never closed, and so the stress is some value lower than the final pressure of 2200 psi.

The compliance method stress estimate is 237-310 psi lower than the SIMFIP estimates. The tangent method stress estimate is even lower, but because the test ended before a tangent point was reached, we do not know how low it would have been.

The mismatch between the SIMFIP and compliance interpretations is somewhat surprising because the dP/dG curve has an 'ideal' shape with a clear upward inflection. One possible explanation is that the SIMFIP measured the closure/reopening of the reactivated natural fracture *at the wellbore*, but away from the wellbore, a hydraulic fracture formed off the natural fracture, perpendicular to Shmin, and the DFIT injection measured the closure of this fracture. Based on the natural fracture orientation, if it closed at 2710 psi, that would imply

that the magnitude of the minimum principal stress is 2567 psi which is close to the contact pressure seen in the dP/dG plot. The details of this stress inversion calculation will be provided in a future publication. This issue does not appear to have been present in the E1-I 64 tests because injection created a new fracture, nor in the TV 4100 interval Test 7, because injection appears to have opened a fracture nearly perpendicular to the minimum principal stress.

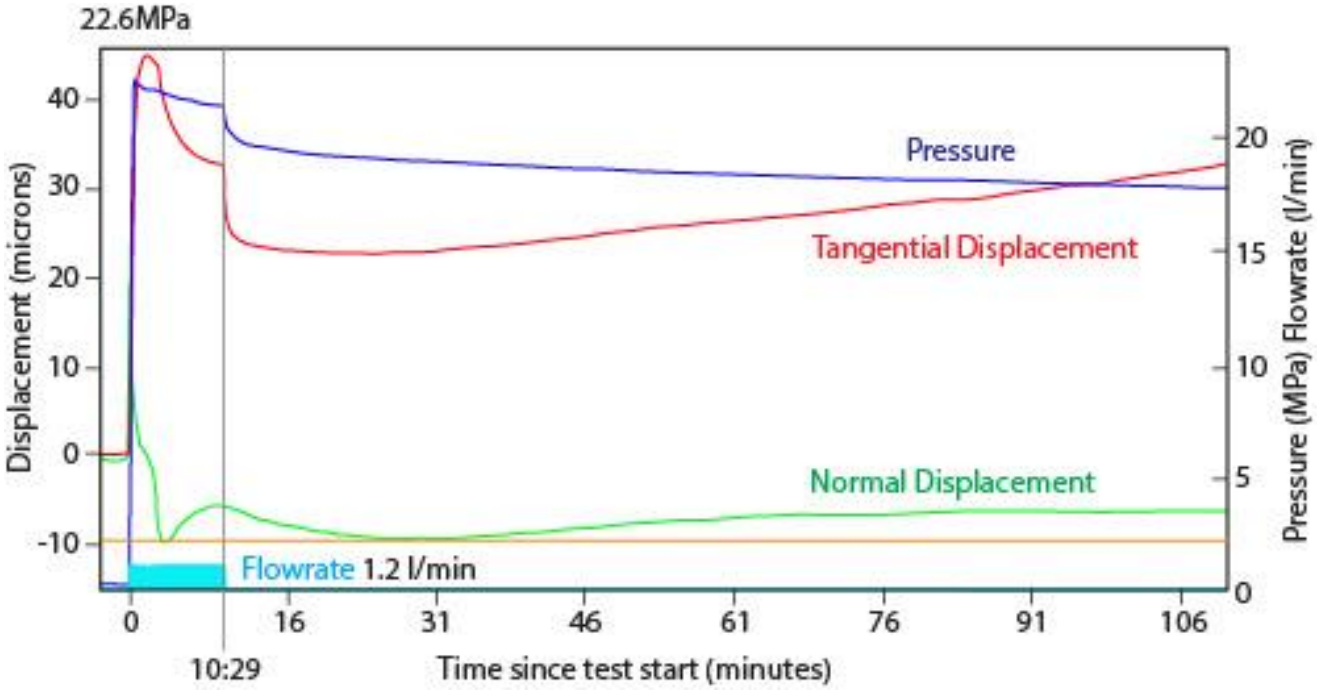

Figure 11: SIMFIP displacement normal and tangential to the activated fracture during TV 4100 Test 4. Displacements are plotted with injection chamber pressure and injection flowrate (note that only a part of the shut-in is plotted on this graph).

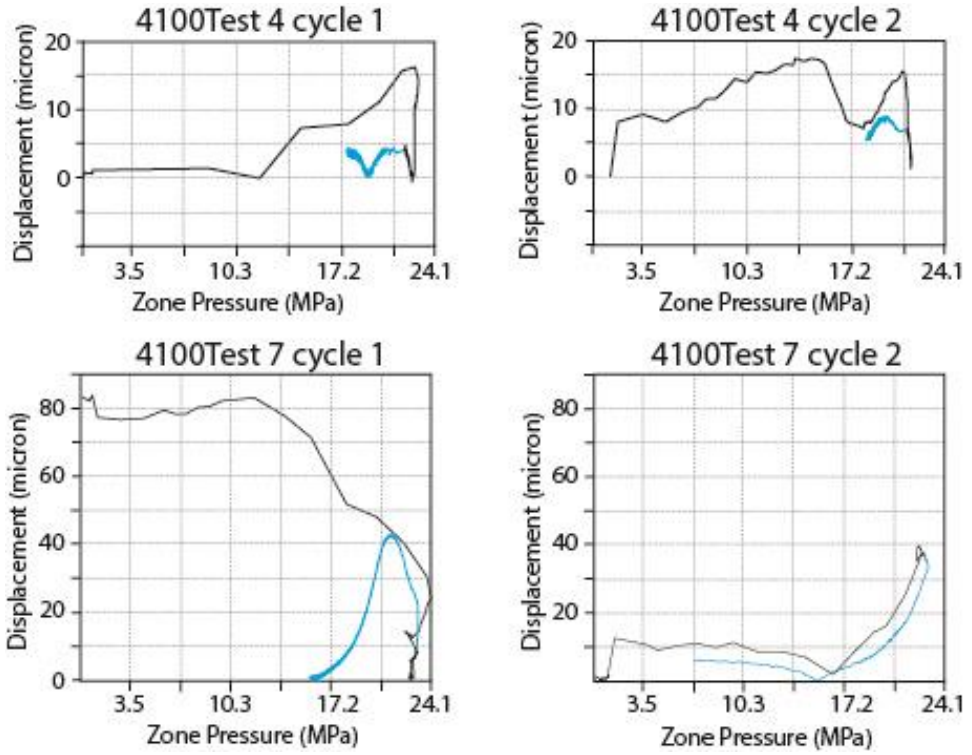

Figure 12: SIMFIP displacement normal to the activated fracture versus zone pressure for the TV 4100 tests (Black is the injection period, blue is the shut-in period).

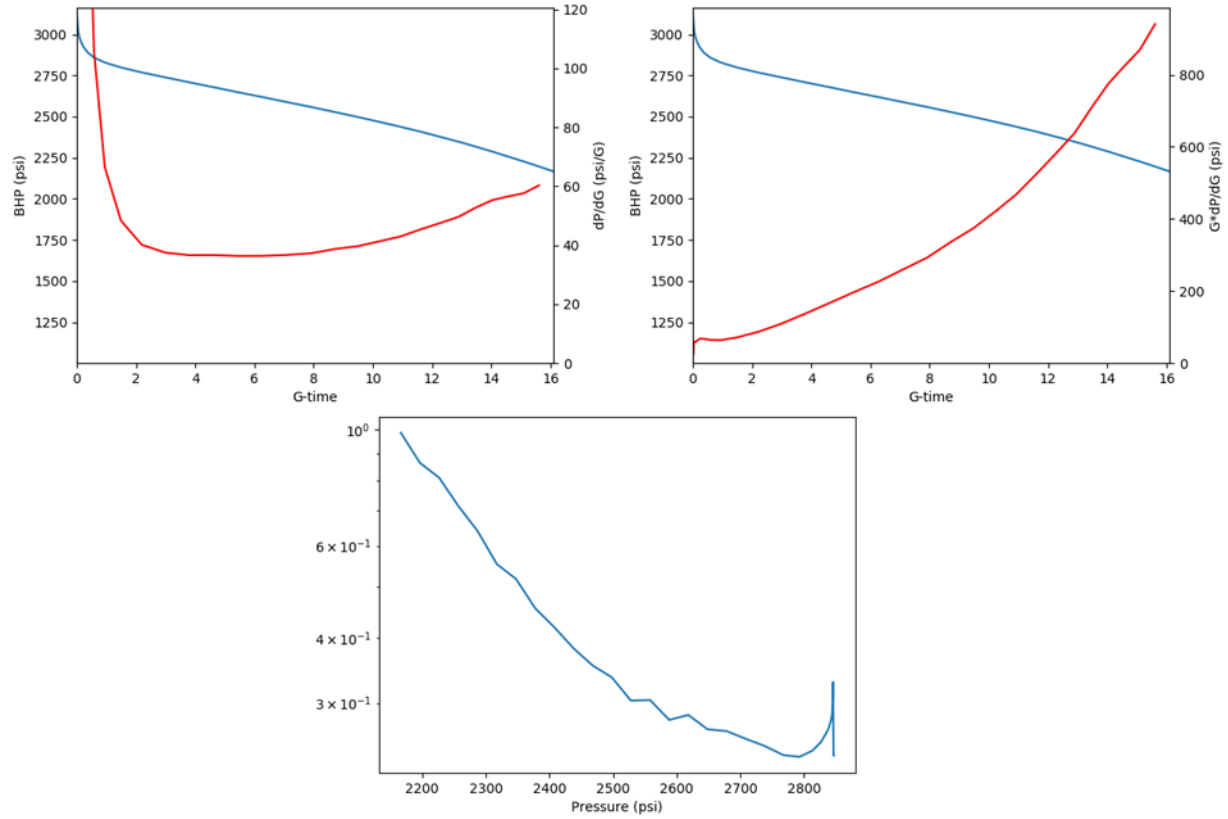

Figure 13: dP/dG, G*dP/dG, and relative stiffness plots for TV 4100 Test 4.

In TV 4100 Test 7, a 12:21 minutes long and 2.8 l/min constant flowrate injection was conducted, followed by a 16-hour overnight shut-in (Figure 14). As in TV 4100 Test 4, it appears that one or several segments of natural fractures reactivated between the SIMFIP anchors. The fracturing pressure is 24.1 MPa. After a complex initial tangential displacement and normal closing, the fracture opens to a maximum of 43 microns. At shut-in there is a smooth variation of fracture opening and shearing.

After shut-in, there is a brief period in which normal displacement continues to increase. Then, the plot of displacement versus pressure settles into a straight line with an x-intercept around 18.5 MPa (2680 psi) (Figure 12). Eventually, the fracture stiffens and closure approaches its asymptotic limit around 16 MPa (2321 psi). During reopening in Cycle 2, displacement lifts off a minimum at 16.4 MPa (2379 psi).

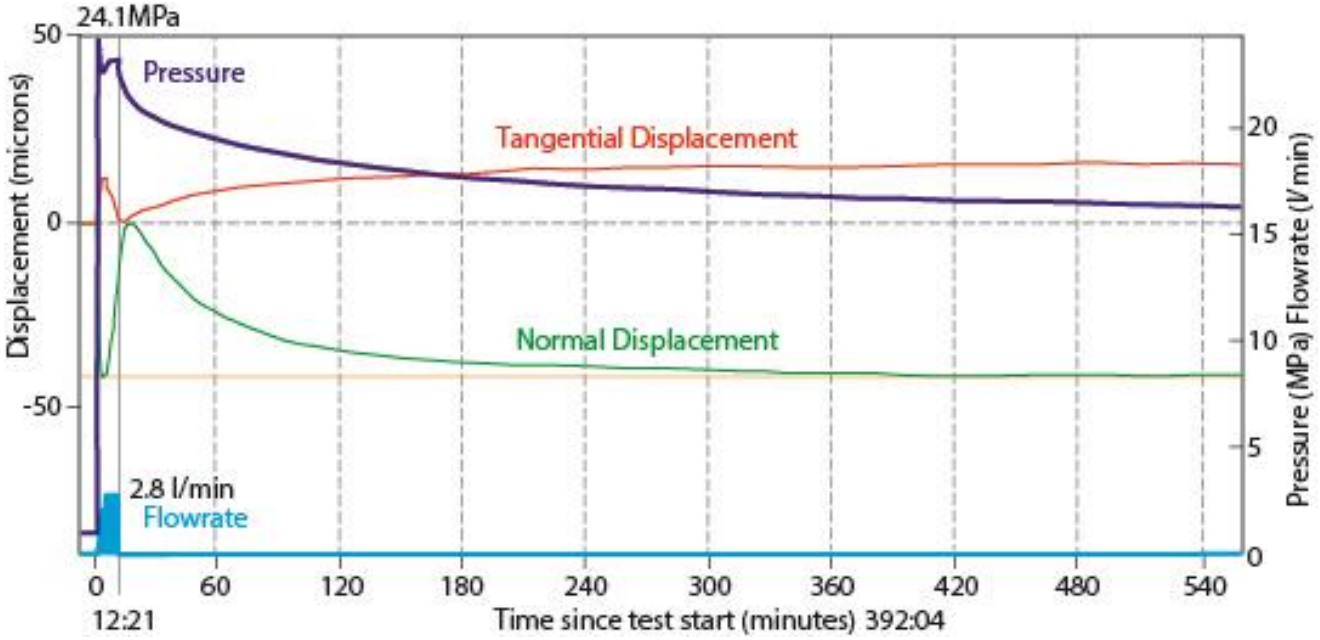

Figure 14: SIMFIP displacement normal and tangential to the activated fracture during TV 4100 Test 7. Displacements are plotted with injection chamber pressure and injection flowrate (note that only a part of the shut-in is plotted on this graph).

At the end of Cycle 2, a flowback was performed. Following Plahn et al. (1997), the closure stress can be estimated from a plot of pressure versus cumulative flowback volume. A straight line is drawn through the linear periods on the plot before and after closure, and the intercept is taken as closure. This procedure yields a closure estimate of around 2700 psi (Figure 15).

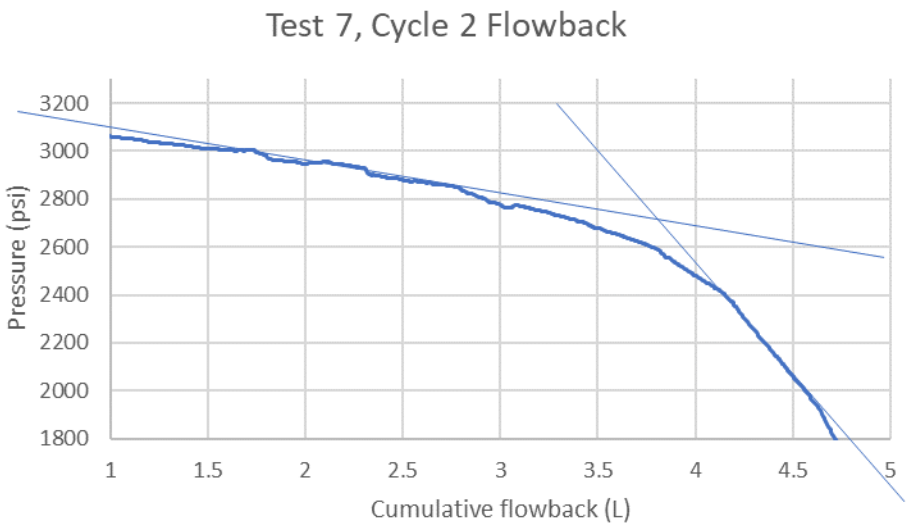

Figure 15: Pressure versus cumulative flowback volume for the TV 4100 Test 7, Cycle 2 flowback.

To summarize, the x-intercept approach from the Cycle 1 shut-in and the flowback interpretation from Cycle 2 suggest a closure estimate around 2680-2700 psi. On the other hand, the point where displacement appears to reach near zero during the Cycle 1 shut-in and the point where displacement lifts off from zero during the Cycle 2 reopening are lower, around 2321-2370 psi. The difference may be that between 2320-2700 psi, the fracture walls are in contact, but the aperture is still significant, due to the roughness of the fracture walls. Or, if the fracture is surrounded by a small damage zone, as mentioned previously, perhaps the cracks close in a complex way.

The dP/dG plot shows what would be termed an 'adequate' indication of closure (McClure et al., 2022). There is an upward deflection in dP/dG, but it never actually reaches a minimum. The upward deflection occurs at approximately 2875 psi, suggesting a stress estimate of 2800 psi. The relative stiffness plot does not show a clear upward inflection, with the implied relative stiffness increasing steadily as pressure drops.

The tangent method closure estimate is around 2700 psi. This is the only test in our dataset where a tangent point was reached prior to the end of shut-in. This is also the only case where the tangent and compliance stress estimates are reasonably similar – within 100 psi.

To recap, the SIMFIP and flowback stress estimates, compliance method stress estimate, and tangent method stress estimates are all within 100 psi (2700-2800 psi), with the compliance estimate slightly higher than the others.

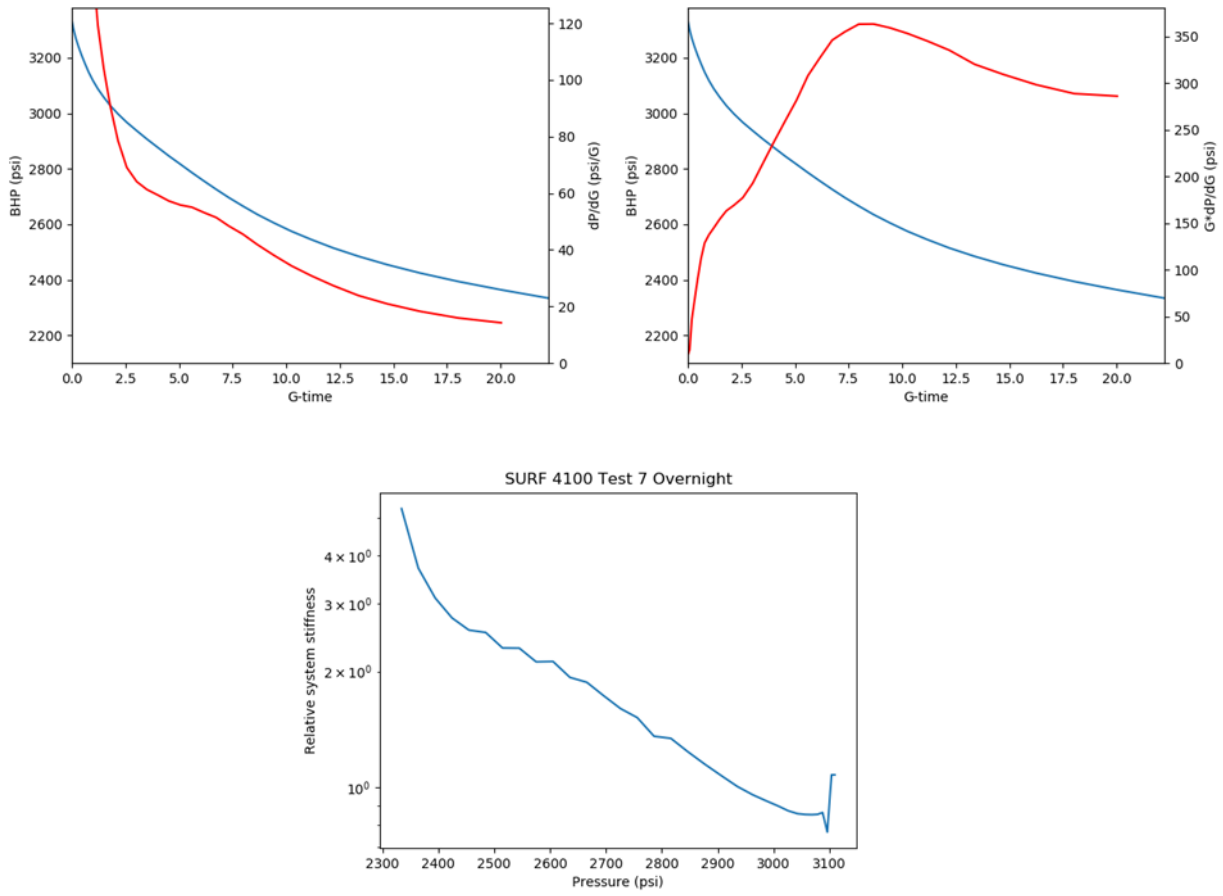

Figure 16: dP/dG, G*dP/dG, and relative stiffness plots for TV 4100 Test 7.

Table 1: Comparison of stress estimates from the tangent method, the compliance method, and the SIMFIP measurements.

Name	Tangent Method (psi)	Compliance Method (psi)	SIMFIP (psi)
E1-I 164 Test 1	Less than 2900	3100	3100
E1-I 164 Test 2	Less than 2200	Rapid closure - 3000-3500	3100
TV 4100 Test 4	Less than 2200	2475	2712 to 2785
TV 4100 Test 7	2700	2800	2700

Table 2: Injection duration, total injection volume, average injection rate, and shut-in duration for the four tests.

Name	Injection duration (min:sec)	Injection volume (L)	Avg Injection rate (L/min)	Shut-in duration (hours)
E1-I 164 Test 1	10:00	2.1	0.21	2
E1-I 164 Test 2	63:00	23	0.37	15
TV 4100 Test 4	10:29	20.5	1.08	7
TV 4100 Test 7	12:21	45.2	2.15	16

4. CONCLUSIONS

1. In three of the four transients, the tangent method estimate is significantly lower than the stress measured by the SIMFIP. In these three tests, the G*dP/dG curve did not reach a tangent point, and so the tangent method interpretation is that the fracture had not closed by the end of the test. In the fourth transient (TV 4100 Test 7), the tangent method and the compliance method yielded values within 100 psi of each other. In this transient, the tangent method result was the same as the SIMFIP estimate.
2. The compliance method estimate from E1-I 164 Test 1 was the same as the SIMFIP measurement. The E1-I 164 Test 2 transient had a monotonically decreasing dP/dG, and so because there is no indication of near-wellbore tortuosity, the compliance method interpretation is 'rapid closure.' This is consistent with the SIMFIP measurement, which predicted closure within several hundred psi of the ISIP. In the TV 4100 Test 4 transient, the compliance closure pick was a few hundred psi lower than the SIMFIP closure pick (albeit, higher and closer to the SIMFIP value than the tangent method interpretation). However, the test opened a natural fracture at the wellbore that was not perpendicular to the minimum principal stress. If the magnitude of Shmin is calculated from the orientation of the natural fracture, then the SIMFIP estimate for Shmin is similar to the compliance closure pick. In the TV 4100 Test 7 transient, the compliance pick was 100 psi higher than the SIMFIP pick.
3. Overall, the results are consistent with findings from McClure et al. (2016), Dutler et al. (2020), and Broker and Ma (2022) that the tangent method interpretation is often far lower than Shmin. The compliance method interpretations are reasonably accurate. However, the compliance method is affected by the frequent occurrence of monotonic dP/dG in lower volume tests, which results in a less precise and more uncertain estimate. In the cases when monotonic dP/dG is observed in the absence of near-wellbore tortuosity, results are supportive of the 'rapid closure' interpretation.
4. Direct in-strain strain measurements are invaluable because they enable 'ground truthing' of cheaper, more available methods of estimating stress. There is a need for additional studies like this one, repeating these experiments in different lithologies and geologic settings.

ACKNOWLEDGEMENTS

This material was based upon work supported by the U.S. Department of Energy, Office of Energy Efficiency and Renewable Energy (EERE), Office of Technology Development, Geothermal Technologies Office, under Award Number DE-AC02-05CH11231 with LBNL, by Lawrence Livermore National Laboratory under Contract DE-AC52-07NA27344, and other awards to other national laboratories. The United States Government retains, and the publisher, by accepting the article for publication, acknowledges that the United States Government retains a non-exclusive, paid-up, irrevocable, world-wide license to publish or reproduce the published form of this manuscript, or allow others to do so, for United States Government purposes. The research supporting this work took place in whole or in part at the Sanford Underground Research Facility in Lead, South Dakota. The assistance of the Sanford Underground Research Facility and its personnel in providing physical access and general logistical and technical support is gratefully acknowledged.

REFERENCES

Barree, R. D., V. L. Barree, and D. P. Craig. 2009. Holistic fracture diagnostics: Consistent interpretation of prefrac injection tests using multiple analysis methods. SPE 107877. SPE Production & Operations 24(3): 396-406.

Barree, R. D., and H. Mukherjee. 1996. Determination of pressure dependent leakoff and its effect on fracture geometry. SPE 36424. Paper presented at the 71st Annual SPE Technical Conference and Exhibition, Denver, CO.

Bröker, Kai, and Xiaodong Ma. 2022. Estimating the Least Principal Stress in a Granitic Rock Mass: Systematic Mini-Frac Tests and Elaborated Pressure Transient Analysis. Rock Mechanics and Rock Engineering. 391.

Castillo, J. L. 1987. Modified fracture pressure decline analysis including pressure-dependent leakoff. SPE 16417. Paper presented at the SPE/DOE Low Permeability Reservoir Symposium, Denver, CO.

Craig, D. P., R. D. Barree, N. R. Warpinski, and T. A. Blasingame. 2017. Fracture closure stress: Reexamining field and laboratory experiments of fracture closure using modern interpretation methodologies. SPE 187038. Paper presented at the SPE Annual Technical Conference and Exhibition, San Antonio, TX.

Cramer, D. D. and D. H. Nguyen. 2013. Diagnostic fracture injection testing tactics in unconventional reservoirs. SPE 163863. Paper presented at the SPE Hydraulic Fracturing Technology Conference, Woodlands, TX.

Delaney, Paul T., David D. Pollard, Joseph I. Ziony, and Edwin H. McKee. 1986. Field relations between dikes and joints: emplacement processes and palesostress analysis. Journal of Geophysical Research 91 (B5): 4920-4938.

Dutler, Nathan, Benoit Valley, Valentin Gischig, Mohammadreza Jalali, Bernard Brixel, Hannes Krietsch, Clement Roques, and Florian Amann. 2020. Hydromechanical insight of fracture opening and closure during in-situ hydraulic fracturing in crystalline rock. International Journal of Rock Mechanics and Mining Sciences 135.

Fu, Pengcheng, et al. 2021. Close observation of hydraulic fracturing at EGS Collab Experiment 1: Fracture trajectory, microseismic interpretations, and the role of natural fractures. Journal of Geophysical Research 126(7): e2020JB020840.

Godbey, J. K., H. D. Hodges. 1958. Pressure measurements during formation fracturing operations. Petroleum Transactions, AIME 213: 65-69

Guglielmi, Yves, Frederic Cappa, Hervé Lançon, Jean Bernard Janowczyk, Jonny Rutqvist, C. F. Tsang, and J. S. Y. Wang. 2013. ISRM Suggested Method for Step-Rate Injection Method for Fracture In-Situ Properties (SIMFIP): Using a 3-Components Borehole Deformation Sensor. Rock Mechanics and Rock Engineering 47: 303-311.

Guglielmi, Y., Nussbaum, C., Rutqvist, J., Cappa, F., Jeanne, P, & Birkholzer, J. 2020. Estimating perturbed stress from 3-D borehole displacements induced by fluid injection in fractured or faulted shales. Geophys. J. Int. (2020) 221, 1684–1695. doi: 10.1093/gji/ggaa103.

Gugliemi, Y., P. Cook, F. Soom, M. Schoenball, P. Dobson, and T. Kneafsey. 2021. In situ continuous monitoring of borehole displacements induced by stimulated hydrofracture growth. Geophysical Research Letters 48.

Gulrajani, Sunil N. and K. G. Nolte. 2000. Chapter 9: Fracture Evaluation using Pressure Diagnostics. In Reservoir Stimulation, eds, Michael J. Economides and Kenneth G. Nolte, Wiley.

Haimson, Bezalel, Charles Fairhurst. 1967. Initiation and extension of hydraulic fractures in rocks. Society of Petroleum Engineers Journal 7 (3), doi: 10.2118/1710-PA.

Hickman, Stephen H., Mark D. Zoback. 1983. The interpretation of hydraulic fracturing pressure-time data for in-situ stress determination. In Hydraulic Fracturing Measurements, ed. M. D. Zoback and B. C. Haimson, 44-54. Washington D.C., National Academy Press.

Hubbert, M. K., D. G. Willis. 1957. Mechanics of hydraulic fracturing. Journal of Petroleum Technology 9 (6): 153-168.

Jaeger, John, N. G. Cook, and Robert Zimmerman. 2017. Fundamentals of Rock Mechanics. 4th Edition. Wiley-Blackwell.

Kakurina, M., Y. Guglielmi., C. Nussbaum, and B..Valley. 2020. In Situ Direct Displacement Information on Fault Reactivation During Fluid Injection. Rock Mechanics and Rock Engineering 53:4313–4328 https://doi.org/10.1007/s00603-020-02160-w.

Kehle, Ralph O. 1964. The determination of tectonic stresses through analysis of hydraulic well fracturing. Journal of Geophysical Research 69 (2): 259-273, doi: 10.1029/JZ069i002p00259.

Kneafsey, T. J., D. Blankenship, H. A. Knox, T. C. Johnson, J. B. Ajo-Franklin, P. C. Schwering, P. F. Dobson, J. P. Morris, M. D. White, P. Fu., R. Podgorney, L. Huang, B. Johnston, W. Roggenthen, T. Doe, E. Mattson, A. Ghassemi, C. Valladao, and the EGS Collab team. 2019. EGS Collab Project: Status and Progress. In *Proceedings of the 44th Workshop on Geothermal Reservoir Engineering*, Stanford University, 16 p.

Kneafsey, T. J., D. Blankenship, P. F. Dobson, J. P. Morris, M. D. White, P. Fu, P. C. Schwering, J. B. Ajo-Franklin, L. Huang, M. Schoenball, T. C. Johnson, H. A. Knox, G. Neupane, J. Weers, R. Horne, Y. Zhang, W. Roggenthen, T. Doe, E. Mattson, C. Valladao, and the EGS Collab team. 2020. The EGS Collab project: Learnings from Experiment 1. *Proceedings, 45th Workshop on Geothermal Reservoir Engineering*, Stanford University, 15 p.

Mack, Mark G., and Norman R. Warpinski. 2000. Mechanics of Hydraulic Fracturing. In Reservoir Stimulation, edited by Michael Economides and Kenneth Nolte.

Malik, Mayank, Ken Schwartz, Ken Moelhoff, and Vinay K. Mishra. 2014. Microfracturing in tight rocks: a Delaware Basin case study. Paper SPE-169009-MS.

McClure, Mark. 2019. Discussion of the Paper "SPE-187038-MS: Fracture Closure Stress: Reexamining Field and Laboratory Experiments of Fracture Closure Using Modern Interpretation Methodologies." arXiv:1904.07126

McClure, Mark W., Hojung Jung, Dave D. Cramer, and Mukul M. Sharma. 2016. The fracture compliance method for picking closure pressure from diagnostic fracture injection tests. SPE Journal 21 (4): 1321-1339, doi: 10.2118/179725-PA.

McClure, Mark, Vidya Bammidi, Craig Cipolla, Dave Cramer, Lucas Martin, Alexei A Savitski, Dave Sobernheim, and Kate Voller. 2019. A Collaborative Study on DFIT Interpretation: Integrating Modeling, Field Data, and Analytical Techniques. Paper presented at the Unconventional Resources Technology Conference, Denver, Colorado.

McClure, Mark, Garrett Fowler, and Matteo Picone. 2022. Best practices in DFIT interpretation: Comparative analysis of 62 DFITs from nine different shale plays. Paper SPE-205297-MS presented at the SPE International Hydraulic Fracturing Technology Conference and Exhibition.

Nolte, Kenneth. 1979. Determination of fracture parameters from fracturing pressure decline. SPE 8341. Paper presented at the Annual Fall Technical Conference and Exhibition of the Society of Petroleum Engineers, Las Vegas, NV.

Plahn, S. V., K. G. Nolte, L. G. Thompson, and S. Miska. 1997. A quantitative investigation of the fracture pump-in/flowback test. SPE Production & Facilities 12(1): 20-27.

Schmitt, Douglas R., and Bezalel Haimson. 2017. Hydraulic fracturing stress measurements in deep holes. From Rock Mechanics and Engineering Volume 1, ed. Xia-Ting Feng.

Schoenball, Martin, Jonathan B. Ajo-Franklin, Doug Blankenship, Chengping Chai, Aditya Chakravarty, Patrick Dobson, Chet Hopp, Timothy Kneafsey, Hunter A. Knox, and Monica Maceira. 2020. Creation of a mixed-mode fracture network at mesoscale through hydraulic fracturing and shear stimulation. Journal of Geophysical Research 125(12): e2020JB019807.

Scholz, Christopher H. 2010. A note on the scaling relations for opening mode fractures in rock. Journal of Structural Geology 32, doi: 10.1016/j.jsg.2010.09.007.

Shylapobersky, J. 1985. Energy analysis of hydraulic fracturing. Paper presented at the 26th US Symposium on Rock Mechanics, Rapid City, South Dakota.

Singh, A., M. Zoback, P. F. Dobson, T. J. Kneafsey, M. Schoenball, Y. Guglielmi, C. Ulrich, W. Roggenthen, N. Uzunlar, J. Morris, P. Fu, P. C. Schwering, H. A. Knox, L. Frash, T.W. Doe, H. Wang, K. Condon, B. Johnston and the EGS Collab team. 2019. Slip tendency analysis of fracture networks to determine suitability of candidate testbeds for the EGS Collab hydroshear experiment. Geothermal Resources Council Transactions, 43, 405–424.

Sneddon, I. N. 1946. The distribution of stress in the neighborhood of a crack in an elastic solid. Proceedings of the Royal Society of London Series A 187 (1009): 229-260, doi: 10.1098/rspa.1946.0077.

Wang, H. F., M. Y. Lee, T. Doe, B. C. Haimson, C. M. Oldenburg, and P. F. Dobson. 2017. In-situ stress measurement at 1550-meters depth at the kISMET test site in Lead, S.D. In 51st US Rock Mechanics / Geomechanics Symposium. San Franscisco, California, USA: American Rock Mechanics Association, ARMA 2017–0651, 7 p.

Zoback, Mark. 2007. Reservoir Geomechanics. Cambridge University Press.